Synergistic effect of trimethylsilane for photoinduced electron transfer on 1,8-naphthalimides in polar solvent

ARTICLE *in* JOURNAL OF PHOTOCHEMISTRY AND PHOTOBIOLOGY A: CHEMISTRY · OCTOBER 2012

Impact Factor: 2.5 · DOI: 10.1016/j.jphotochem.2012.07.008

Journal of Photochemistry and Photobiology A: Chemistry 246 (2012) 23–28

Contents lists available at SciVerse ScienceDirect

Journal of Photochemistry and Photobiology A: Chemistry

journal homepage: www.elsevier.com/locate/jphotochem

Synergistic effect of trimethylsilane for photoinduced electron transfer on 1,8-naphthalimides in polar solvent

Dae Won Cho[a,*], Dae Won Cho[b], Hea Jung Park[c], Ung Chan Yoon[c], Myoung Hee Lee[a], Chan Im[a,d,**]

[a] Konkuk University – Fraunhofer ISE Next Generation Solar Cell Research Center, Konkuk University, Seoul 143-701, Republic of Korea
[b] Department of Chemistry, Yeungnam University, Gyeongsan 712-749, Republic of Korea
[c] Department of Chemistry, Pusan National University, Pusan 609-734, Republic of Korea
[d] Department of Chemistry, Konkuk University, Seoul 143-701, Republic of Korea

ARTICLE INFO

Article history:
Received 7 March 2012
Received in revised form 22 May 2012
Accepted 18 July 2012
Available online xxx

Keywords:
1,8-Naphthalimide
Photoinduced electron transfer
Transient absorption spectroscopy
DFT calculation

ABSTRACT

Photoinduced electron-transfer (PET) process of 1,8-naphthalimide—linker—TMS (NI—SOS—TMS, where SOS = dithiaoxaundecyl and TMS = trimethylsilane) has been investigated using transient absorption measurements in CH_3CN and CH_3CN/H_2O (v/v = 9:1). The femtosecond pulsed laser excitation of NI—SOS—TMS produced the NI radical anion ($NI^{\bullet -}$) with a transient absorption band around 415 nm, via the intramolecular PET from heteroatom nearby TMS to NI in the singlet excited (S_1) state. However, in case of NI—SOS, the transient band at around 415 nm increased concomitantly with the decay of $^1NI^*$ (or $^3NI^*$) at around 470 nm. This is implied that $NI^{\bullet -}$ is primarily generated via the intermolecular quenching of $^1NI^*$ (or $^3NI^*$) by NI. In contrast, in a protic polar solvent mixture of CH_3CN/H_2O, a proton abstraction process occurred from $NI^{\bullet -}$ to generate the NI ketyl radical ($NIH^{\bullet}$), which showed a transient absorption band around 405 nm. The decay time constants of $NIH^{\bullet}$ were quite long compared to those of $NI^{\bullet -}$ in CH_3CN. Both the rates of charge transfer and deactivation processes of transient species largely depended on the protic polar solvent.

1. Introduction

Phthalimides are well-known electron-acceptor substrates that undergo photoinduced electron-transfer (PET) reactions with olefins, amines, and electron-rich alkyl benzenes to produce the corresponding radical anions, which subsequently abstract protons from either the solvent or quenchers [1]. The photocyclization reactions of trimethylsilyl-terminated poly-heteroatom donor-linked phthalimides have been investigated extensively [2,3]. These reactions have proven to be highly efficient methods for preparing polyethers, thioethers, sulfonamides, and cyclic peptides. Most photocyclization reactions have been carried out in pure or mixed protic polar solvents. Though protic polar solvents show the effects of hydrophilic interactions, hydrogen bonding, and proton transfer coupled with the PET process, the role of protic polar solvents in the photocyclization reaction has not been fully examined.

1,8-Naphthalimides (NI) have likewise attracted considerable interest because of their photophysical properties and potential applications in various scientific fields, such as photobiology [4–7]. In many studies, NI derivatives have been used for the investigation of PET between DNA as an electron donor and NI as an electron acceptor. The PET mechanisms in DNA or biomaterial systems are of intrinsic interest because the reactions take place in aqueous or partially aqueous environments. We have been studying the role of protons in the PET mechanism for NI dyads and *bis*-NI systems [8,9]. In protic polar solvent, the NI radical anions ($NI^{\bullet -}$) generated from the PET process undergo proton abstraction to produce the ketyl radical species ($NIH^{\bullet}$) of NI in CH_3CN/H_2O.

The covalently linked NI dyads with electron donor sites are often used to mimic PET processes in natural systems [10,11]. Several electron donors can be introduced into NI-dyads. Among these, an organosilane is a unique electron donor in photocyclization reactions [12]. Although there is no direct evidences, based on photoproduct analysis, $NIH^{\bullet}$ species has been suggested as an intermediate in photocyclization process.

In the present study, we examine the photoreduced intermediates of NI derivatives in aprotic as well as protic polar solvents using transient absorption measurements. For the study, NI dyad that has a linker between trimethylsilane (TMS) and the electron-accepting NI moieties (NI—SOS—TMS, where SOS is 3,9-dithia-6-oxaundecyl) was prepared (Scheme 1). Thioether (—SOS—) have lower oxidation

* Corresponding author. Tel.: +82 2 450 0404.
** Corresponding author at: Konkuk University – Fraunhofer ISE Next Generation Solar Cell Research Center, Konkuk University, Seoul 143-701, Republic of Korea. Tel.: +82 2 450 0404.
E-mail addresses: dwcho@konkuk.ac.kr (D.W. Cho), chanim@konkuk.ac.kr (C. Im).

1010-6030/$ – see front matter © 2012 Elsevier B.V. All rights reserved.
http://dx.doi.org/10.1016/j.jphotochem.2012.07.008

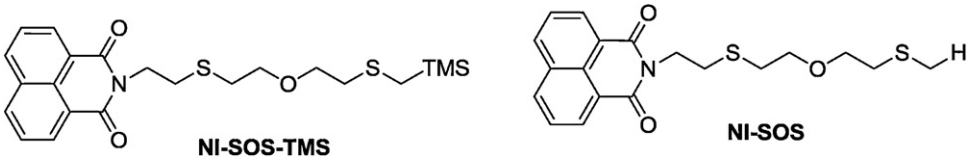

Scheme 1. Molecular structures.

potential compared with polyalkyl group [13,14]. The photocyclization reactions of NIs that contain internal thioether donor sites (O or S) are chemically efficient (80–100%) and that they take place exclusively by a pathway involving sequential PET biradical cyclization [15]. Therefore, we also introduced thioether linker in order to investigate the role of TMS in intramolecular PET process. We also synthesized reference NI molecule such as NI—SOS, which was not trimethylsilylated (Scheme 1).

Based on the transient absorption spectroscopic results, we concluded that the $NI^{\bullet-}$ in NI—SOS—TMS is generated by the intramolecular PET process. In case of NI—SOS, the $NI^{\bullet-}$ is generated by intermolecular PET process. Moreover, $NI^{\bullet-}$ is converted to the NIH• species in protic polar solvent. Density functional theory (DFT) calculation results were compared with experimental observations.

2. Experimental

2.1. Synthesis

N-(10-trimethylsilanyl-3,9-dithia-6-oxaundecyl)-1,8-naphthalimide (NI—SOS—TMS) was synthesized as follows.

NI—SOS—TMS. To a tetrahydrofuran solution containing 1,8-naphthalimide (0.59 g, 3.0 mmol), 10-tetramethylsilanyl-3,9-dithia-6-oxaundecyl iodide [16] (0.67 g, 2.5 mmol), and PPh_3 (0.78 g, 3.0 mmol) was added diisopropyl azodicarboxylate (DIAD) (0.59 g, 3.0 mmol); the solution was stirred for 12 h at room temperature. After evaporation *in vacuo*, hexane was added to crystallize the residue. The crystallized solid was removed and the final solution was concentrated *in vacuo* to give a residue that was subjected to column chromatography (CH_2Cl_2) to yield 0.72 g (64%). ^{1}H NMR ($CDCl_3$) 0.07 (s, 9H, $SiMe_3$), 1.83 (s, 2H, CH_2SiMe_3), 2.71 (t, 2H, SCH_2, J = 7.2 Hz), 2.84–2.93 (m, 4H, SCH_2), 3.64–3.72 (m, 4H, OCH_2), 4.39 (t, 2H, NCH_2, J = 7.5 Hz), 7.74 (dd, 2H, aromatic, J = 7.5 and 7.8 Hz), 8.21 (d, 2H, aromatic, J = 8.1 Hz), 8.58 (d, 2H, aromatic, J = 7.2 Hz); ^{13}C NMR ($CDCl_3$) −1.8, 18.9, 29.8, 31.5, 35.3, 39.7, 70.1, 70.4, 122.5, 126.9, 128.2, 131.3, 131.6, 134.0, 164.0; HRMS (FAB) *m*/*z* 447.6921 (M+H, $C_{22}H_{29}NO_3S_2Si$ requires 447.6861).

The detailed synthesis of NI—SOS has been described earlier [10,17].

2.2. Spectroscopic measurements

Steady-state absorption and fluorescence spectra were measured using an UV–vis spectrophotometer (Sinco, Neosys-2000) and a fluorophotometer (Sinco, FS-2), respectively. The fluorescence quantum yields were measured by an absolute PL quantum yield spectrometer (Hamamatsu, Quantaurus-QY C11347-01).

Time-resolved fluorescence spectra were measured by the single photon counting method, using a streak scope (Hamamatsu Photonics, C10627-03) equipped with a polychromator (Acton Research, SP2300). An ultrashort laser pulse was generated with a Ti:sapphire oscillator (Coherent, Vitesse, FWHM 100 fs) pumped with a diode-pumped solid-state laser (Coherent, Verdi). High-power (1.5 mJ) pulses were generated with a Ti:sapphire regenerative amplifier (Coherent, Libra, 1 kHz). For excitation of the sample, the output of the Ti:sapphire regenerative amplifier was converted to 330 nm by an optical parametric amplifier (Coherent, TOPAS). The instrument response function was also determined by measuring the scattered laser light to analyze a temporal profile. This method gives a time resolution of about 50 ps after the deconvolution procedure. The temporal emission profiles were well-fitted into a single-exponential function. The residuals were less than 1.1 for each system.

The sub-picosecond time-resolved absorption spectra were collected by a pump-probe transient absorption spectroscopy system (Ultrafast Systems, Helios) [18]. The pump light was generated by using a regeneratively amplified titanium sapphire laser system (Coherent, Libra-F, 1 kHz) pumped by a diode-pumped Q-switched laser (Coherent, Evolution). The seed pulse was generated by a titanium sapphire laser (Coherent, Vitesse). The pulse (330 nm) generated from an optical parametric amplifier (Coherent, TOPAS) was used as the excitation pulse. And a white light continuum pulse, which was generated by focusing the residual of the fundamental light to a thin CaF_2 crystal after the computer-controlled optical delay, was used as a probe beam and directed to the sample cell with 1.0 mm of optical path and detected with the CCD detector installed in the absorption spectroscopy. The pump pulse was chopped by the mechanical chopper synchronized to one-half of the laser repetition rate, resulting in a pair of the spectra with and without the pump, from which absorption change induced by the pump pulse was estimated.

Nanosecond transient absorption measurements were carried out by the technique of laser flash photolysis. The samples were excited using the 355 nm pulses of the third harmonic generation from a Q-switched Nd:YAG laser (Continuum, Surelite II-10, pulse width of 4.5 ns FWHM). A xenon lamp (ILC Technology, PS 300-1) was focused on the sample solution as the probe light for the transient absorption measurements. The transient absorption spectra were measured by an intensified charge-coupled device (ICCD, Ando, iStar). Temporal profiles were measured with a monochromator (DongWoo Optron, Monora 500i) equipped with a photomultiplier (Zolix Instruments Co., CR 131) and a digital oscilloscope (Tektronix, TDS-784D). Reported signals were averages of 200 events. All solutions were argon-saturated unless otherwise indicated.

3. Results and discussion

3.1. Steady-state absorption and emission properties

The absorption and fluorescence spectra of NI—SOS—TMS in aprotic CH_3CN and protic CH_3CN/H_2O (v/v = 9:1) are shown in Fig. 1. The absorption and emission spectra of NI—SOS—TMS in CH_3CN showed vibronic structure, but the spectra in CH_3CN/H_2O were less structured. The absorption and fluorescence maxima of NI—SOS—TMS in CH_3CN/H_2O shifted slightly to longer wavelength, as compared to those in CH_3CN. The spectral parameters of NI—SOS—TMS are listed in Table 1. The energy levels of the lowest singlet excited state $^1(\pi,\pi^*)$ and second triplet excited state $^3(n,\pi^*)$ of NI are close in nonpolar solvents [19]. In aprotic polar solvent, the energy of $^3(n,\pi^*)$ decreases and that of $^1(\pi,\pi^*)$ slightly increases. Therefore, the energy gap between $^1(\pi,\pi^*)$ and $^3(n,\pi^*)$ increases

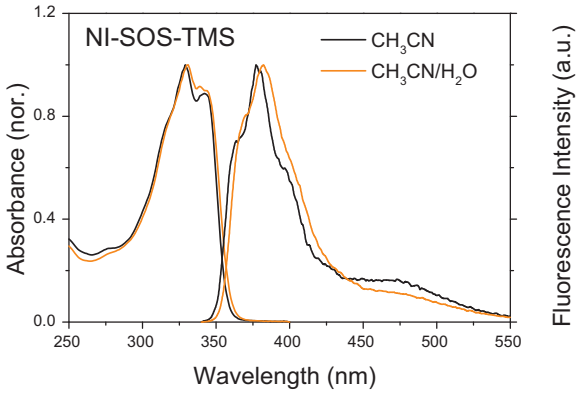

Fig. 1. Absorption and fluorescence spectra of NI—SOS—TMS in CH_3CN and CH_3CN/H_2O. Excitation wavelength is 330 nm.

Table 1
Absorption and fluorescence maxima of NI derivatives in CH_3CN and CH_3CN/H_2O.

	In CH_3CN (nm)		In CH_3CN/H_2O (nm)	
	Abs	Em	Abs	Em
NI—SOS—TMS	329, 343	377	330	382
NI—SOS	331, 345	380	332	383

and mixing of the two states will be less important. Moreover, the protic polar solvent forms a hydrogen bond with the excited molecule. Its effects on $^1(\pi,\pi^*)$ and $^3(n,\pi^*)$ are similar to those induced by increasing the solvent polarity. Consequently, the fluorescence quantum yields (ϕ_f) increases in protic polar solvents. This effect is clearly observed in the present NI derivatives. The ϕ_f for NI—SOS—TMS and NI—SOS molecules in CH_3CN/H_2O were larger than those in CH_3CN (Table 2). Based on the above results, we can conclude that NI is surrounded by H_2O in both ground and excited state. It is noteworthy that the emission quantum yields of NI—SOS—TMS were reduced compared to those of the reference NI—SOS in both solvents.

In CH_3CN, the fluorescence lifetime (τ_f) in the singlet excited state ($^1NI^*$) were measured to be 0.17 ns for NI—SOS—TMS, while that for the reference NI—SOS was measured as 0.27 ns as listed in Table 2. $^1NI^*$ had longer lifetime in CH_3CN/H_2O than in CH_3CN. This trend was consistent with the enhancement of quantum yield in CH_3CN/H_2O. Especially, the τ_f values for NI—SOS—TMS were much shorter than those of the reference NI—SOS compounds in both solvents.

From the τ_f values, the deactivation rate constant (k_S) of $^1NI^*$—SOS—TMS in CH_3CN was determined to be $5.9 \times 10^9\ s^{-1}$, which was substantially larger than that of the corresponding reference NI—SOS ($3.7 \times 10^9\ s^{-1}$). In addition, the ϕ_f of $^1NI^*$—SOS—TMS decreased in comparison to that of the reference NI—SOS (Table 2). Thus, these behaviors strongly suggested that the diminished fluorescence resulted from rapid PET from SOS—TMS to $^1NI^*$ to give $NI^{\bullet-}$—$(SOS—TMS)^{\bullet+}$.

Table 2
Fluorescence lifetimes (τ_f) and quantum yields (ϕ_f) of NI derivatives in CH_3CN and CH_3CN/H_2O solutions.[a]

	In CH_3CN			In CH_3CN/H_2O		
	τ_f (ns)	ϕ_f	ε_{ET}	τ_f (ns)	ϕ_f	ε_{ET}
NI—SOS—TMS	0.17	0.013	0.37	0.18	0.015	0.66
NI—SOS	0.27	0.025	–	0.53	0.062	–

[a] Excitation wavelength is 330 nm.

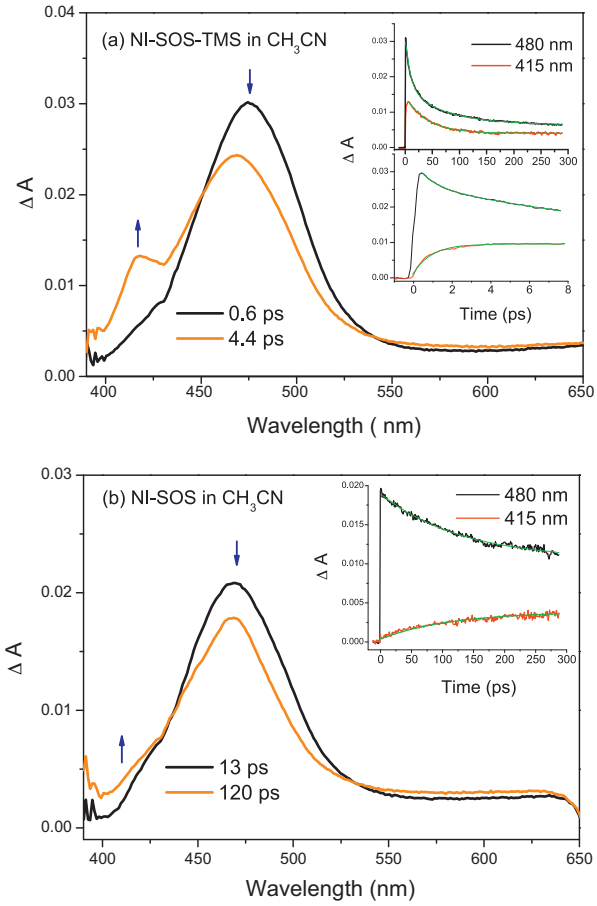

Fig. 2. Transient absorption spectra of (a) NI—SOS—TMS, and (b) NI—SOS observed various time delays after a pulse excitation with 130 fs pulse at 330 nm in CH_2CN. The inset shows the kinetic trace of ΔA at 480 and 415 nm.

The PET efficiencies (ε_{ET}) in the S_1 state were determined as 37% for NI—SOS—TMS in CH_3CN, respectively, using Eq. (1) [20]:

$$\varepsilon_{ET} = 1 - \frac{\tau_{DA}}{\tau_A} \quad (1)$$

where τ_A and τ_{DA} represent the emission lifetimes of the electron acceptor (NI) and of electron donor (SOS—TMS), respectively. In protic polar CH_3CN/H_2O, the PET for NI—SOS—TMS was about twofold more efficient than that of NI—SOS—TMS in CH_3CN.

3.2. Transient absorption characteristics

Fig. 2 shows the transient absorption spectra of NI—SOS—TMS and NI—SOS in CH_3CN. Upon excitation of NI—SOS—TMS with 130 fs pulse at 330 nm, a transient absorption bands were observed around 465 nm. This band can be assigned to S_1–S_n absorption band of NI [21]. On the other hand, a transient absorption band at 415 nm increased gradually according to time delay. This band can be assigned to $NI^{\bullet-}$ [11]. As shown in inset decay profiles of Fig. 2a, the formation time constant of $NI^{\bullet-}$ in CH_3CN was 0.93 ps monitored at 415 nm, which is faster than the fluorescence lifetimes of 170 ps for $^1NI^*$—SOS—TMS. It is concluded that the PET process in the hot vibrational level of S_1 state can occur, and then $NI^{\bullet-}$ species is in the equilibrium with $^1NI^*$ species. In CH_3CN/H_2O, the PET process for $^1NI^*$—SOS—TMS take placed in 0.69 ps as shown in Fig. S1a in supplementary content. This result indicates that the TMS group plays an inductive role as the electron donor of SOS linker in PET process. We suggest that the intramolecular PET

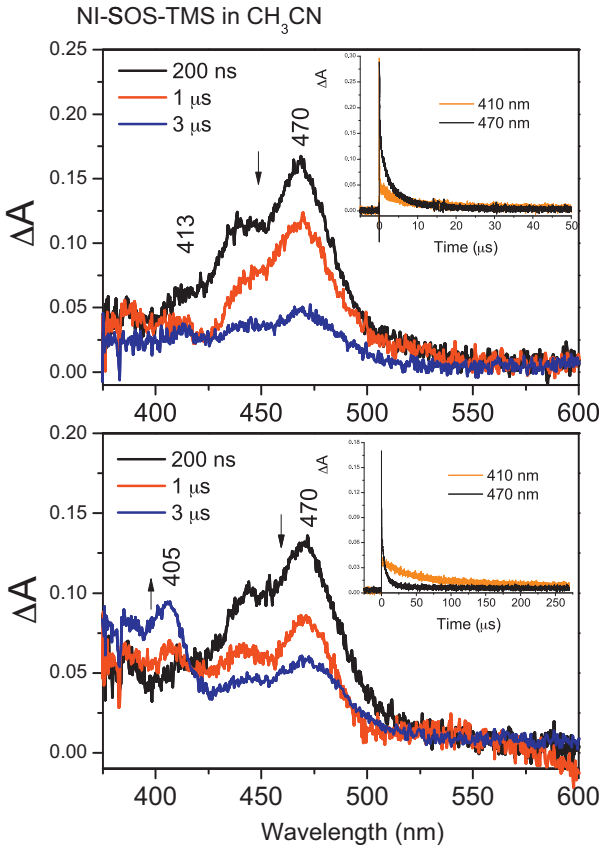

Fig. 3. Transient absorption spectra of NI—O_3—TMS in (a) CH_3CN, and (b) CH_3CN/H_2O. Inserts show the decay profiles monitored at 470 and 410 nm (or 405 nm), respectively. Excitation wavelength was 355 nm.

mechanism for NI—SOS—TMS as following:

$$\text{NI-SOS-TMS} \xrightarrow{h\nu} {}^1\text{NI}^*\text{-SOS-TMS} \xrightarrow{\text{PET}} \text{NI}^{\bullet-}\text{(-SOS-TMS)}^{\bullet+} \xrightarrow{H_2O} \text{NI(H)}^{\bullet}\text{(-SOS-TMS)}^{\bullet+} \quad (2)$$

On the other hand, it is noteworthy that the growth of $NI^{\bullet-}$ transient bands for NI—SOS at 415 nm occurs concomitantly with the decay of the S_1–S_n absorption at 480 nm (inset in Fig. 2b). This indicates that the $NI^{\bullet-}$ species produced after formation of $^1NI^*$ which is precursor of $NI^{\bullet-}$ species having an absorption at 415 nm. The quenching mechanism of $^3NI^*$ by using another NI was previously suggested [8,9,22,23]. The driving force for PET from S_1 state is larger than from T_1 state. Therefore, we suggest the intermolecular PET mechanism for reference NI—L derivatives and NI—O_3—TMS as following:

$$\text{N} \xrightarrow{h\nu} {}^1\text{NI}^* \xrightarrow{\text{ISC}} {}^3\text{NI}^* \quad (3)$$

$${}^1\text{NI}^* + \text{NI} \xrightarrow{\text{PET}} \text{NI}^{\bullet-} + \text{NI}^{\bullet+} \xrightarrow{H_2O} \text{NI(H)}^{\bullet} + \text{NI}^{\bullet+} \quad (4)$$

Based on fs-transient absorption studies for NI—SOS—TMS, we can conclude that the intramolecular PET occurs in both aprotic and protic polar solutions. However, the intermolecular PET mainly occurs in NI—SOS in both solvents.

The ns-transient absorption spectra of NI derivatives were obtained by nanosecond-laser flash photolysis measurement with 355-nm laser excitation. Fig. 3 shows the transient absorption spectra of NI—SOS—TMS (3×10^{-5} M) measured in CH_3CN and CH_3CN/H_2O under the argon saturated condition. The transient absorption spectra of NI—SOS—TMS in CH_3CN showed a characteristic band around 470 nm, which might correspond to the T_1–T_n absorption of NI in the triplet excited state ($^3NI^*$) [8,10,11]. The transient band at 415 nm can be attributed to $NI^{\bullet-}$, according to previous reports [10,11,24].

Table 3
Decay time constants of triplet-state (τ_T), anion radical (τ_A) and ketyl radical (τ_K) species in CH_3CN and CH_3CN/H_2O.

	In CH_3CN		In CH_3CN/H_2O		In CH_3CN/D_2O	
	τ_T (μs)	τ_A (μs)	τ_T (μs)	τ_K (μs)	τ_T (μs)	τ_K (μs)
NI—SOS—TMS	0.26	6.6	0.31	56	0.30	13

In CH_3CN, the transient absorption of NI—SOS—TMS decayed with first-order kinetics as illustrated in the inset of Fig. 3(a); the decay lifetime of $^3NI^*$—SOS—TMS were estimated to be 0.26 μs, at the 470-nm wavelength (Table 3). At the 410-nm wavelength, the decay lifetimes of NI—SOS—TMS was 6.6 μs, which was attributed to the charge recombination (CR) process between $NI^{\bullet-}$ and the cation radical moieties. There is no rise component corresponding to the decay of $^3NI^*$ at 470 nm. These observations mean that the PET process takes place from the excited singlet state in CH_3CN. On the other hand, the transient absorption spectrum of NI—SOS in CH_3CN also showed a T_1–T_n absorption band at 470 nm, but the absorption band at 410 nm is not clear.

In CH_3CN/H_2O, the T_1–T_n absorption of NI—SOS—TMS was observed at 470 nm, with weak transient absorption bands at 415 and 405 nm (Fig. 2(b)). The transient band at 405 nm can be attributed to $NI(H)^{\bullet}$, according to previous reports [10,11,24]. In addition, the transient absorption bands showed different kinetic traces, as shown in the inset of Fig. 2(b). The T_1–T_n absorption at 470 nm decayed with a lifetime of 0.31 μs. On the other hand, the transient absorption at 405 nm showed an initial formation and then a very slow decay with a lifetime of 56 μs.

In CH_3CN/D_2O (v/v = 9:1), the T_1–T_n absorption of NI—SOS—TMS was observed at 470 nm, with weak transient absorption bands at around 410 nm (Fig. S2 in supplementary content). The transient band at 405 nm can be assigned to $NI(D)^{\bullet}$. The T_1–T_n absorption at 470 nm decayed with a lifetime of 0.30 μs. On the other hand, the transient absorption at 405 nm showed an initial formation and then a slow decay with a lifetime of 13 μs. On the other hand, NI—SOS in CH_3CN/D_2O also showed a T_1–T_n absorption band at 470 nm which is decayed with a lifetime of 0.81 μs, but the transient absorption band at 410 nm is not clear (Fig. S2 in supplementary content).

The PET for NI—L was mainly influenced by the heteroatoms in the linkers. The free energy change (ΔG_{PET}) associated with electron transfer can be evaluated using the following equation:

$$\Delta G_{ET} = e(E_{ox}{}^0 - E_{red}{}^0) - E_{00} - \frac{e^2}{\varepsilon_s r} \quad (5)$$

where $E_{ox}{}^0$ and $E_{red}{}^0$ are oxidation and reduction potentials for the donor and acceptor, respectively, and E_{00} denotes the excitation energy. The last term is the Coulombic term, which is the work required to bring the donor and acceptor to the electron-transfer distance, with e being the unit charge; r, the distance between the acceptor and donor; and ε_s, the static dielectric constant of the polar solvents. Generally, the last term is less than 0.01 eV. The reduction potential of 1,8-naphthalimide was reported as −1.44 V vs. SCE in CH_3CN [19]. The excitation energies of the excited singlet and triplet states of NI were reported as 3.4 [5,19,25] and 2.3 eV [19,24], respectively. On the other hand, the oxidation potential of thioether (—S—) was reported as 1.4 V [14]. Based on the above parameters, the driving force (ΔG_{PET}) for PET between the donor and acceptor can be calculated. The driving force of NI—SOS—TMS is −0.56 eV in the excited singlet state. This indicates that the PET process could take place in NI—SOS—TMS in the excited singlet state.

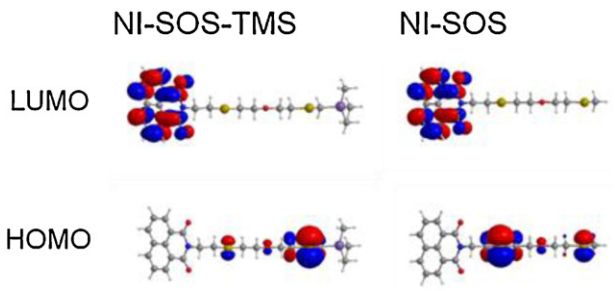

Fig. 4. HOMO and LUMO orbital diagrams for NI—SOS—TMS and NI—SOS calculated by B3LYP function with 6–31G(d) basis.

For NI—SOS—TMS, on the other hand, it is well known that a α-trialkylsilyl substituent in heteroatom-containing electron donors has a profound effect on their oxidation potentials [26,27]. For example, a substantial lowering of oxidation potential by (trimethylsilyl)methyl substitution was observed in aromatic systems [28]. Therefore, the PET process in NI—SOS—TMS can be carried out efficiently through the inductive effects of TMS.

The transient absorption band at 405 nm in protic polar solvent can be attributed to NIH•, according to previous works [8,9,29]. The ketyl radical species of naphthalimide or phthalimides have been suggested as intermediates in photocyclization reactions with a lack of direct evidence [12]. The ketyl radical is electrically neutral and not a charged species, therefore, the regeneration process of NI derivatives is slow. Thus, the transient absorption band at 405 nm shows a longer decay time of a few tens of microseconds. The long lifetime of the ketyl radical is beneficial for the photocyclization reaction from the collision-opportunity point of view.

3.3. Analysis of HOMO and LUMO orbitals

Fig. 4 shows the HOMO and LUMO orbitals of NI—SOS—TMS and NI—SOS, which were performed with the Gaussian 03 program suite. The geometries were optimized by the density function theory (DFT) method using Becke's three-parameter hybrid exchange functional with the Lee–Yang–Parr correlation function (B3LYP), employing the 6–31G(d) level in vacuum. The HOMO of NI—SOS—TMS and NI—SOS are located on the S atoms of linker. The HOMO orbital of NI—SOS is largely populated on S atom close to NI moiety. In NI—SOS—TMS, however, the S atom proximal to the TMS group has a large electron density. On the other hand, the LUMO orbitals for NI—SOS—TMS and NI—SOS possess a high electron density on the NI moiety and there is a lower distribution of electron density on the linkers compared to the HOMO. This denoted the charge transfer from the heteroatoms of linker to the NI moiety in the excited state. As shown in Fig. 4, the LUMO orbitals remain basically the same, independent of the linkers. The HOMO orbitals showed different electronic distributions which may influence to the oxidation potentials of linkers. Therefore, one would need to calculate in detail the time-dependent DFT, and the interaction with protic polar solvents to obtain information which might be consistent with the experimental finding along the series of NI compounds.

4. Conclusions

In this work, the transient species of NI—SOS—TMS were investigated using the femtoscond- and nanoscond-transient absorption spectroscopic techniques. The photophysical properties of NI—SOS—TMS were compared with those of NI—SOS. The primary intramolecular PET process for NI—SOS—TMS was observed between NI and SOS—TMS linker in the excited singlet state. However, in case of NI—SOS, the intermolecular PET process may take place. In protic polar solvent, the proton abstraction process occurred from $NI^{\bullet -}$ to generate the NI ketyl radical (NIH•), which exhibited a long lifetime. From the calculation, the electron of the HOMO level of NI—SOS—TMS was largely delocalized in the heteroatoms near TMS, and the electron of the LUMO orbital was predominately distributed in the NI moiety. This theoretical result shows the strong probability in the PET from the L—TMS to the NI moiety.

Acknowledgments

This work has been supported by a Grant-in Aid for the Seoul R&BD Program (WR090671), and Solar Energy Industrial R&D Exchange and Cooperation Project (2011) from Seoul Metropolitan Government, and a National Research Foundation of Korea (NRF) grant funded by the Korea government (MEST) (No. 2010-0027660).

Appendix A. Supplementary data

Supplementary data associated with this article can be found, in the online version, at http://dx.doi.org/10.1016/j.jphotochem.2012.07.008.

References

[1] Y. Konaka, K. Sakai, R. Murata, Y. Hatanaka, Photoaddition reactions of N-methylphthalimide with toluenes and amines, Heterocyles 3 (1975) 719–722.
[2] U.C. Yoon, P.S. Mariano, The synthetic potential of phthalimide SET photochemistry, Accounts of Chemical Research 234 (2001) 523–533.
[3] U.C. Yoon, Y.X. Jin, S.W. Oh, C.H. Park, J.H. Park, J.H. Campana, X. Cai, E.N. Duesler, P.S. Mariano, A synthetic strategy for the preparation of cyclic peptide mimetics based on the SET-promoted photocyclization processes, Journal of the American Chemical Society 125 (2003) 10664–10671.
[4] I. Saito, M. Takayama, H. Sugiyama, K. Nakatani, A. Tsuchida, M. Yamamoto, Photoinduced DNA cleavage via electron transfer: demonstration that guanine residues located 5′ to guanine are the most electron-donating sites, Journal of the American Chemical Society 117 (1995) 6406–6407.
[5] J.E. Rogers, L.A. Kelly, Nucleic acid oxidation mediated by naphthlene and benzophenone imide and diimide derivatives: consequences for DNA redox chemistry, Journal of the American Chemical Society 121 (1999) 3854–3861.
[6] K. Kawai, Y. Osakada, E. Matsutani, T. Majima, Charge separation and photosensitized damage in DNA mediated by naphthalimide, naphthaldiimide, and anthraquinone, Journal of Physical Chemistry B 114 (2010) 10195–10199.
[7] T. Takada, Y. Takeda, M. Fujitsuka, T. Majima, "Signal-On" detection of DNA hole transfer at the single molecule level, Journal of the American Chemical Society 131 (2009) 6656–6657.
[8] D.W. Cho, M. Fujitsuka, U.C. Yoon, T. Majima, Intermolecular photoinduced electron-transfer of 1,8-naphthalimides in protic polar solvents, Physical Chemistry Chemical Physics 10 (2008) 4393–4399.
[9] D.W. Cho, M. Fujitsuka, A. Sugimoto, T. Majima, Intramolecular excimer formation and photoinduced electron transfer process in bis-1,8-naphthalimide dyads depending on the linker length, Journal of Physical Chemistry A 112 (2008) 7208–7213.
[10] D.W. Cho, M. Fujitsuka, A. Sugimoto, U.C. Yoon, P.S. Mariano, T. Majima, Photoinduced electron transfer processes in 1,8-naphthalimide-linker-phenothiazine dyads, Journal of Physical Chemistry B 110 (2006) 11062–11068.
[11] (a) D.C. Jagesar, S.M. Fazio, J. Taybi, E. Eiser, F.G. Gatti, D.A. Leigh, A.M. Brouwer, Photoinduced shuttling dynamics of rotaxanes in viscous polymer solutions, Advanced Functional Materials 19 (2009) 3440–3449;
(b) D.W. Cho, M. Fujitsuka, U.C. Yoon, T. Majima, Intermolecular exciplex formation and intramolecular electron transfer during photoirradiation of 1,8-naphthalimide–linker–phenothiazine dyads in methylated benzenes, Journal of Photochemistry and Photobiology A: Chemistry 190 (2007) 101–109.
[12] D.W. Cho, U.C. Yoon, P.S. Mariano, Studies leading to the development of a single-electron transfer (SET) photochemical strategy for syntheses of macrocyclic polyethers, polythioethers, and polyamides, Accounts of Chemical Research 44 (2011) 204–215.
[13] Estimated based on oxidation potentials of alcohols given in Lund. Electroorganic preparations. II. Oxidation of carbinols, Acta Chemica Scandinavica 11 (1957) 491–498.
[14] P. Cottrell, C.K. Mann, Electrochemical oxidation of aliphatic sulfides under nonaqueous conditions, Journal of the Electrochemical Society 116 (1969) 1499–1503.
[15] U.C. Yoon, H.C. Kwon, T.G. Hyung, K.H. Choi, S.W. Oh, S. Yang, Z. Zhao, P.S. Mariano, The photochemistry of polydonor-substituted phthalimides: curtin-hammett-type control of competing reactions of potentially interconverting

zwitterionic biradical intermediates, Journal of the American Chemical Society 126 (2004) 1110–1124.
[16] U.C. Yoon, S.W. Oh, J.H. Lee, J.H. Park, K.T. Kang, P.S. Mariano, Applications of phthalimide photochemistry to macrocyclic polyether, polythioether, and polyamide synthesis, Journal of Organic Chemistry 66 (2001) 939–943.
[17] D.W. Cho, M. Fujitsuka, K.H. Choi, M.J. Park, U.C. Yoon, T. Majima, Intramolecular exciplex and intermolecular excimer formation of 1,8-naphthalimide–linker–phenothiazine dyads, Journal of Physical Chemistry B 110 (2006) 4576–4582.
[18] D.W. Cho, M. Fujitsuka, J.H. Ryu, M.H. Lee, H.K. Kim, T. Majima, C. Im, S2 emission from chemically modified BODIPYs, Chemical Communications 48 (2012) 3424–3426.
[19] V. Wintgens, P. Valet, J. Kossanyi, L. Biczók, A. Demeter, T. Bérces, Spectroscopic properties of aromatic dicarboximides. Part 1. —N—H and N-methyl-substituted naphthalimides, Journal of the Chemical Society, Faraday Transactions 90 (1994) 411–421.
[20] J.R. Lakowicz, Principles of Fluorescence Spectroscopy, 3rd edition, Springer Science, Singapore, 2006 (Chapter 13).
[21] A. Smanta, G. Saroja, Steady state and time-resolved studies on the redox behaviour 1,8-naphthalimide in the excited state, Journal of Photochemistry and Photobiology A: Chemistry 84 (1994) 19–26.
[22] B.M. Aveline, S. Matsugo, R.W. Redmond, Photochemical mechanisms responsible for the versatile application of naphthalimides and naphthaldiimides in biological systems, Journal of the American Chemical Society 119 (1997) 11785–11795.
[23] H.-Q. Li, Z.-Q. Jiang, X. Wang, Y. Pan, F. Wang, S.-O. Yu, Study on electron transfer of a novel 1,8-naphthalimide probe and nucleosides by laser flash photolysis, Research on Chemical Intermediates 30 (2004) 369–381.
[24] G. Jones II, S. Kumar, Participation of chromophore pairs in photoinduced intramolecular electron transfer for a naphthalimide spermine conjugate, Journal of Photochemistry and Photobiology A: Chemistry 160 (2003) 139–149.
[25] J.E. Rogers, S.J. Weiss, L.A. Kelly, Photoprocesses for naphthalene imide and diimide derivatives in aqueous solutions of DNA, Journal of the American Chemical Society 122 (2000) 427–436.
[26] J. Yoshida, T. Maekawa, T. Murata, S. Matsunaya, S. Isoe, Electrochemical oxidation of organosilicon compounds. Part 7. The origin of β-silicon effect in electron-transfer reactions of silicon-substituted heteroatom compounds. Electrochemical and theoretical studies, Journal of the American Chemical Society 112 (1990) 1962–1970.
[27] J. Yoshida, S. Matsunaga, T. Murata, S. Isoe, New one carbon homologation reagents utilizing electrochemical oxidation of organosilicon compounds, Tetrahedron 47 (1991) 615–624.
[28] B.E. Cooper, W.J. Owen, Silicon, α-Carbon hyperconjugation in cation radicals: I. Lowering of oxidation potentials of N-[(trimethylsilyl)methyl] aromatic amines, Journal of Organometallic Chemistry 29 (1971) 33–40.
[29] A. Demeter, L. Biczók, T. Bérces, V. Wintgens, P. Valat, J. Kossanyi, Laser photolysis studies of transient processes in the photoreduction of naphthalimides by aliphatic amines, Journal of Physical Chemistry 97 (1993) 3217–3224.